Accurate Wavenumbers for Mid-Infrared Fine-Structure Lines

Douglas M. Kelly^{1,2} and John H. Lacy¹

Department of Astronomy, University of Texas, Austin, TX 78712 email: dkelly@kaya.uwyo.edu

To be Published in The Astrophysical Journal Letters

¹Visiting Astronomer at the Infrared Telescope Facility, which is operated by the University of Hawaii under contract to the National Aeronautics and Space Administration.

 $^{^2\}mathrm{Current}$ Address: Department of Physics and Astronomy, University of Wyoming, Laramie, WY 82071-3905

ABSTRACT

We present accurate new wavenumbers for a set of 13 mid-infrared fine-structure lines. The wavenumbers were determined from observations of the planetary nebula NGC 7027 and of the red supergiant α Scorpii. Most of the new wavenumbers are good to within 0.0025%, or 8 km s⁻¹. We provide details on the measurements and present an analysis of the errors. In addition, we present the first observations of hyperfine splitting in the [Na IV] 1106 cm⁻¹ line.

Subject headings: atomic data — infrared: ISM: lines and bands — planetary nebulae: individual (NGC 7027)

1. Introduction

The strongest features in the mid-infrared spectra of gaseous nebulae are the fine-structure lines of [Ne II], [S III], [S IV], and [Ar III] and the series of unidentified PAH or carbon grain features. This set of atomic and solid state features has been the center of attention for most mid-infrared galaxy studies to date, and it represents the general limit of what can be detected in galaxies from the ground with 4-meter class telescopes (e.g. Roche et al. 1991; Kelly et al. 1995). However, with the impending launch of the Infrared Space Observatory (ISO) and with the development of 8-meter class, infrared-optimized telescopes, new opportunities are unfolding in the field of mid-infrared spectroscopy.

ISO will be capable of observing a large number of lines in bright galaxies, including many lines which have never been detected before except in novae. In most galaxies, however, the number of detectable lines will be relatively small so it will be inefficient to get complete spectral coverage. It is therefore essential to have accurate wavenumbers for the lines of interest. In the course of this study, we have found that predicted wavenumbers can be in error by as much as several tenths of a percent. Thus, in support of the ISO mission and of our own ground-based programs, we have undertaken a project to determine accurate new wavenumbers for fine-structure lines in the mid-infrared. Our target for most of these observations has been the hot, young planetary nebula NGC 7027. This planetary nebula is unusual in that the central star has a temperature of roughly 2×10^5 K (Kaler & Jacoby 1989), but it is still surrounded by a neutral, molecular cloud (see Graham et al. 1993). The kinematics and morphologies of the various ions in NGC 7027 could be quite different from each other, and the extended, complicated nature of NGC 7027 is the major source of our wavenumber uncertainties.

2. Observations

We measured a variety of fine structure lines in the mid-infrared spectrum of NGC 7027 during observing runs at the NASA Infrared Telescope Facility (IRTF) in 1992 August, 1993 June, and 1994 October. The observations were made using Irshell, a mid-infrared grating spectrometer (Lacy et al. 1989; Achtermann 1994). Irshell has an 11x64 pixel Si:As array, with 11 rows in the spatial direction and 64 columns in the spectral direction. We used a low dispersion grating in 1992 August to measure the entire 8-13 μ m spectrum of NGC 7027 at a resolution of $\lambda/\Delta\lambda \approx 1000$. We switched to an echelle grating to measure individual lines during the 1993 June and 1994 October runs. The dispersion of the echelle observations ranged from 16000-25000 (depending on the grating angle), and with a 2 pixel slit width (2'' on the 3m IRTF), the resulting resolution ranged from 8000-12500. A dome-temperature card, chopped against the sky, was used for flatfielding, atmospheric correction, and fluxing (Lacy et al. 1989). For the 1994 October run, we installed a test-grade Hughes 20x64 pixel Si:As array. The 20x64 array has slightly smaller pixels, and the October 1994 data were measured through a 2 pixel (1.6'')wide slit at a resolution of 9500-15000. We used the bright star μ Cephei (spectral type M2Ia; Hoffleit & Jaschek 1982) for flatfielding, atmospheric correction, and fluxing of our 1994 October data.

The ideal approach to this project would be to make spectral maps of each of the lines, and we made such a map for the [S III] line in 1993 June (see Figure 1). With these data cubes, we could register the spatial and spectral positions of the line emission, which would give us the best chance at determining the rest frame wavenumber of the emission. As a bonus, we would also get line intensities and kinematic information. However, since time was limited, we had to make a number of compromises. First, we observed at only one slit position for each line. Since we did not cover the entire source, our information on line strengths was limited to one-dimensional line intensity profiles. Second, we did not have the time to be precise in our pointing. Our usual practice was to move our N-S slit back and forth a few arcseconds E-W across the western emission lobe until we found the maximum signal. Our pointing varied because of guiding and tracking errors and because the morphologies of the various ions are not identical. Third, we rarely measured calibration star spectra. The card calibration is adequate in most cases, but a star spectrum is helpful for removing strong telluric features. Fourth, we speeded up our observations by opening the slit to two arcseconds even though we could have improved our resolution by using a slightly narrower slit. Fifth, we did not make long observations. We spent 2-5 minutes on each of the strong lines and no more than fifteen minutes on the fainter lines. In Section 3, we discuss the effects of these compromises on the accuracy of our wavenumbers.

The most important result from this paper are the vacuum rest wavenumbers of the lines. These values are presented in Table 1, along with estimated 1σ uncertainties (see Section 3) and relative intensities. Of particular note are the three hyperfine components of [Na IV] at 1106 cm⁻¹ (see Section 6). The reasonable agreement between the observational wavenumbers and the wavenumbers predicted by Kaufman & Sugar (1986) and Wiese et al. (1966) gives us confidence in our line identifications. We present a summary of our wavenumber coverage and non-detections in Table 2. Spectra for the lines detected in NGC 7027 are presented in Figure 2. The spectra are usually set to zero in regions of very poor atmospheric transmission (<15 %). All data were reduced using the Snoopy data reduction program (Achtermann 1992).

3. Uncertainties in Wavenumber Measurements

The main sources of error in our wavenumber measurements are summarized below. These contributions were summed in quadrature to determine the uncertainties listed with the wavenumbers in Table 1. For convenience, we quote errors in km s⁻¹, i.e. as fractions of the wavenumber.

1. The wavenumber calibration and when possible the dispersion of the mid-infrared spectra were determined from the atmospheric lines. We determined the centroids of the atmospheric features from our off-position nod frames, and we were able to determine the centroids to within $0.5 - 2 \text{ km s}^{-1}$. The errors introduced by our dispersion solution were always less than 1 km s^{-1} .

2. We obtained wavenumbers for the atmospheric lines from the AFGL line list (McClatchey et al. 1973), and the wavenumbers are good to well under 1 km s⁻¹. However, the atmospheric lines are often blended, and their relative strengths depend on atmospheric conditions, so there is some uncertainty in the effective wavenumbers determined from atmospheric models. When we had to calibrate our wavenumber scale from a blend of atmospheric features, our uncertainties ranged up to 4 km s⁻¹.

3. Photon noise led to scatter in the measured wavenumbers of the individual emission lines. It is almost impossible to determine the magnitude of this effect because of the velocity structure of NGC 7027, but we estimate that the errors are negligible for the strong lines and up to 4 km s⁻¹ for the weaker lines. Since most line measurements involve the averaging of detections at several positions along the slit, the photon noise is reduced and is expected to contribute no more than 2 km s⁻¹ to the wavenumber uncertainties.

4. The lines in NGC 7027 do not have simple line profiles. There is often emission at more than one velocity from a given position in the nebula. We had limited success at deconvolving the line profiles, so we instead determined centroids for the lines. We were able to measure line centroids that were accurate to $0.5 - 1 \text{ km s}^{-1}$. In some cases, bad flatfielding altered the line profiles. In these cases our line centroids could be off by as much as 5 km s⁻¹. The trio of lines at 1106 cm⁻¹ was severely blended, leading to 3 - 6 km s⁻¹ of uncertainty in the line positions.

5. We hinge our velocity reference frame on the [S III] line. The 3 km s⁻¹ uncertainty in the [S III] wavenumber is propagated into the error estimate for all of the other lines. The previous best measurements of the [S III] wavenumber were by Baluteau et al. (1976), who found a wavenumber of 534.39 ± 0.01 cm⁻¹ based on measurements of the Orion Nebula, and by Greenberg, Dyal, & Geballe (1977), who found a wavenumber of 534.41 ± 0.03 cm⁻¹ from observations of three planetary nebulae, including NGC 7027. We used three methods to estimate the [S III] wavenumber. First, by measuring the mean wavenumber over the [S III] map and correcting for the heliocentric velocity of 8.8 ± 0.6 km s⁻¹ given by Schneider et al. (1983), we determine an average wavenumber of 534.388 ± 0.004 cm⁻¹. Second, by comparing the intensity and velocity profiles of the [S III] and [Ne II] emission, we find the best match if the [S III] wavenumber is 534.388 ± 0.005 cm⁻¹. The rest wavenumber for [Ne II] was measured in the laboratory by Yamada, Kanamori, & Hirota (1985), and is $780.424 \pm 0.001 \text{ cm}^{-1}$. Third, by comparing the velocities of the bright ridges in our [S III] map to those in the H76 α velocity map by Roelfsema et al. (1991), we determine a wavenumber of $534.387 \pm 0.005 \text{ cm}^{-1}$. These three values combine to form our new [S III] wavenumber estimate of 534.387 ± 0.005 The two [S III] slit positions that pass through the center of the nebula have flux-weighted average velocity shifts of roughly -1 km s⁻¹ relative to the nebular mean.

6. Telescope tracking errors and pointing uncertainties could have a strong influence on our line profiles and measured wavenumbers. We see velocity gradients of as large as 6 km s⁻¹ per arcsecond along the slit, with a total shift of 15 - 20 km s⁻¹ in the line centroids from one end of the slit to the other. In the E-W direction, we see a shift of over 10 km s⁻¹ to the red in the flux-weighted mean wavenumber along the slit as the slit is moved from west to east across the nebula, with most of the shift taking place in the faint outskirts of the nebula. We determined our N-S and E-W positions for each line by comparing the intensity and velocity profiles along the slit to the [S III] intensity and velocity map presented in Figure 1. These comparisons allowed us to determine the slit positions to within 2", which allowed us to remove the velocity offsets relative to the [S III] frame with 2 km s⁻¹ uncertainty. On the basis of these comparisons, we estimate that the velocity uncertainties due to internal motions in NGC 7027 are 2 - 4 km s⁻¹. In cases where there was not enough flux to determine the profile of the line emission along the slit, we estimate our uncertainties to be 4 - 6 km s⁻¹.

4. [Fe II] Measurements in Alpha Scorpii

We observed two [Fe II] lines in the mid-infrared spectrum of the red supergiant α Scorpii. These observations will be discussed by Haas et al. (1996). The wavenumbers were reduced to the rest frame using the heliocentric velocity of -5.0 \pm 0.6 km s⁻¹ determined by Brooke, Lambert, & Barnes (1974) for low-excitation metals in the spectrum of α Scorpii. The wavenumber uncertainties are dominated by uncertainties in the effective wavenumbers of blended atmospheric lines. The [Fe II] wavenumbers are listed in Table 1.

5. Line Intensities

Our slit measurements provide us with intensity measurements for the mid-infrared lines in NGC 7027. As can be seen from the [S III] map in Figure 1, the brightest emission for the low ionization lines comes from the bright ridges to either side of the nebula center (see also Aitken & Roche 1983). Our slit profiles for the higher ionization lines are consistent with their having similar spatial distributions. Since most of our line measurements were made with our N-S slit crossing one or both lobes, we have reasonable estimates for the peak intensities of the lines. These peak intensities are listed in Table 1. It should be emphasized that these intensities do not all refer to identical spatial positions, and there is a factor of two variation in the continuum levels for the various lines. No corrections have been made for extinction. These intensities are provided only as a general guideline to the strengths of mid-infrared lines in photoionized gas. Line ratios using these numbers could easily be off by a factor of two.

6. Hyperfine Splitting of the [Na IV] Line

Since the dominant isotope of sodium, ²³Na, has nuclear spin, we suspect that the group of lines at 1106 cm^{-1} are the hyperfine components of the [Na IV] ${}^{3}P_{2} - {}^{3}P_{1}$ transition, which is predicted to lie near this wavenumber. To test this hypothesis, we calculated the expected hyperfine splitting and relative line intensities. The hyperfine energy splittings are due mainly to the interaction between the magnetic dipole moment of the nucleus and the magnetic field at the nucleus due to the orbital and spin motion of the electrons. There is a secondary contribution due to the interaction between the quadrupole electric field of the nucleus and the electrons. Hyperfine splitting has not previously been observed in $[^{23}Na \text{ IV}]$ but was observed by Harvey (1965) in the isoelectronic atom $[^{17}O I]$. To calculate the [Na IV] hyperfine splittings, we used the fact that both fine-structure and hyperfine structure splittings are proportional to $< r^{-3} >$ to scale from the hyperfine splitting measurements of [¹⁷O I] and the fine-structure splittings of [O I] and [Na IV], taking into account the differing nuclear magnetic dipole and electric quadrupole moments and the fact that the fine-structure splittings are also proportional to Z_i . We calculated the expected line intensities using the formulae presented in Townes & Schawlow (1955). There are eight hyperfine components in four closely spaced groups, from the four hyperfine sublevels of the J=2 fine-structure level. Of these, the two highest wavenumber groups are blended at our resolution, leaving three resolved lines. The resulting spectrum (shown as a dotted curve in the [Na IV] spectrum of Figure 2) agrees remarkably well with the data, confirming our identification of this multiplet of lines.

We note that ²⁵Mg, ³⁹K, and ⁴¹K also have nuclear spin, but the observed ${}^{3}P_{0} - {}^{3}P_{1}$ transitions should have unresolvably small hyperfine splittings. However, the hyperfine splitting of the strong ${}^{3}P_{2} - {}^{3}P_{1}$ (5.6µm) line of [²⁵Mg V] should be resolvable, allowing a determination of the ${}^{25}Mg/{}^{24}Mg$ abundance ratio. Several isotopic K and Cl fine-structure lines may also have resolvable hyperfine structure.

We are very grateful to Matt Richter and Kevin Luhman for their assistance with the observations and to the daycrew at the IRTF for their excellent instrument support. We thank M. Haas, M. Werner, and E. Becklin for allowing us to present the [Fe II] wavenumbers. Special thanks to Jeff Achtermann for developing the Snoopy data reduction software and the DSP-based Linus operating system. This work has been supported by USAF contract F19628-93-K-0011 and by NSF grant AST-9020292.

TABLE 1Fine-Structure Line Measurements

Ion	Transition	Obs. Date	Wavenumber	Peak	χ_{lower}	χ_{upper}
			(cm^{-1})	Intensity ^{a}	(eV)	(eV)
[Fe II]	$a^4F_{5/2} - a^4F_{7/2}$	6-8 Jun 93	$407.84 \pm .02$		7.87	16.18
[Ne V]	${}^{3}P_{0} - {}^{3}P_{1}$	6 Jun 93	$411.256 \pm .006$	1.3(-11)	97.11	126.21
[S III]	${}^{3}P_{1} - {}^{3}P_{2}$	$4 \ \mathrm{Jun} \ 93$	$534.387 \pm .005$	2.6(-12)	23.33	34.83
[Fe II]	$a^4 F_{7/2} - a^4 F_{9/2}$	6-8 Jun 93	$557.50 \pm .02$		7.87	16.18
[Mg V]	${}^{3}P_{1} - {}^{3}P_{0}$	9 Jun 93	$739.581 \pm .012$	1.5(-12)	109.24	141.27
[Ar V]	${}^{3}P_{0} - {}^{3}P_{1}$	$20~{\rm Aug}~92$	$763.23 \pm .05$	1.3(-12)	59.81	75.02
[Ne II]	${}^{2}P_{3/2} - {}^{2}P_{1/2}$	$4 \ \mathrm{Jun} \ 93$	${}^{b}780.4238 {\pm}.001$	2.5(-12)	21.56	40.96
[Na IV]	${}^{3}P_{2(F=7/2)} - {}^{3}P_{1}$	10Jun 93	$1105.88 \pm .02$	3 (-13)	71.64	98.91
	${}^{3}P_{2(F=5/2)} - {}^{3}P_{1}$	10Jun 93	$1106.12 \pm .02$	2(-13)	71.64	98.91
	${}^{3}P_{2(F=3/2)} - {}^{3}P_{1}$	10Jun 93	$1106.30 \pm .03$	1 (-13)	71.64	98.91
	${}^{3}P_{2(F=1/2)} - {}^{3}P_{1}$	10Jun 93			71.64	98.91
[Mg VII]	${}^{3}P_{0} - {}^{3}P_{1}$	10Jun 93	$1110.00 \pm .05$	8 (-14)	186.51	224.95
[Ar III]	${}^{3}P_{2} - {}^{3}P_{1}$	10Jun 93	$1112.176 \pm .015$	5.1(-12)	27.63	40.74
[K VI]	${}^{3}P_{0} - {}^{3}P_{1}$	10 Jun 93	$1132.52 \pm .03$	1.0(-13)	82.66	99.89
[Ar V]	${}^{3}P_{1} - {}^{3}P_{2}$	24 Oct 94	$1265.57 \pm .04$	1.9(-12)	59.81	75.02

 a erg s⁻¹ cm⁻² sr⁻¹; not corrected for extinction; uncertainties can be large (see Section 5) b wavenumber determined from laboratory measurements by Yamada et al. (1985)

	Non-D	etection Sur	mmary	
Target Line	Wavenumber Coverage		Non-Detections	
	(cm)	$^{-1})$		
[Fe II]	406.25 -	408.60		
[Ne V]	410.75 -	413.30	[Ca VI]	411.5^{a}
[S III]	533.8 -	- 535.1		
[Fe II]	556.75 -	- 558.50		
[Mg V]	735.22 -	- 741.1	[Fe III]	739.1
[F V]	742.75 -	- 746.99	[F V]	746.3
[Ar V]	759.66 -	- 767.12	[S V]	767.5^{a}
[Ne II]	778.9 -	- 781.6		
[S III]	831.70 -	- 835.18	[S III]	832.5^{b}
[Cl IV]	848.93 -	- 853.94	[Cl IV]	849.6
[Al VI]	1095.25 -	- 1099.78	[Al VI]	1097.0
[Na IV] +	1104.7 -	- 1113.0		
[Mg VII] +				
[Ar III]				
[K VI]	1129.9 -	- 1133.4		
[Na VI]	1159.33 -	- 1165.20	[Na VI]	1161.4
			[Mg IX]	1162.3^{a}
			[Cl VI]	
[Ar V]	1263.4 -	- 1266.0		
	1268.07 -	- 1270.81		

TABLE 2

^aline is from an excited term and so is expected to be very weak ^belectric quadrupole transition is expected to be very weak

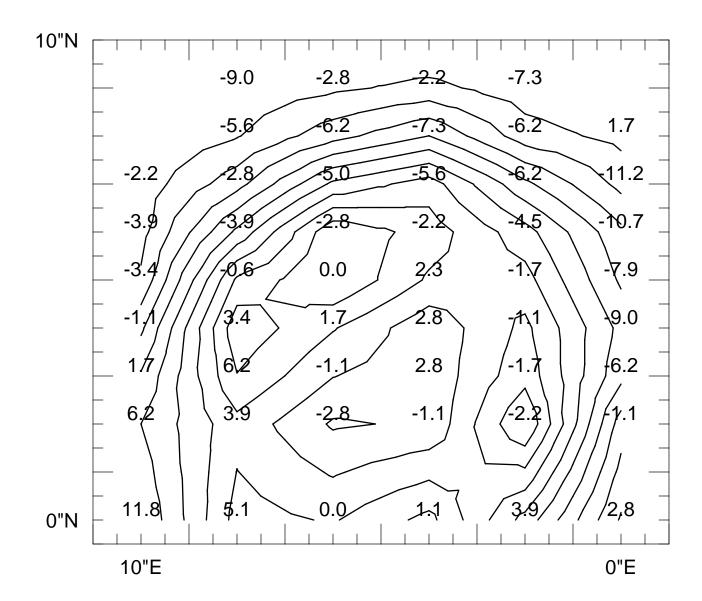
REFERENCES

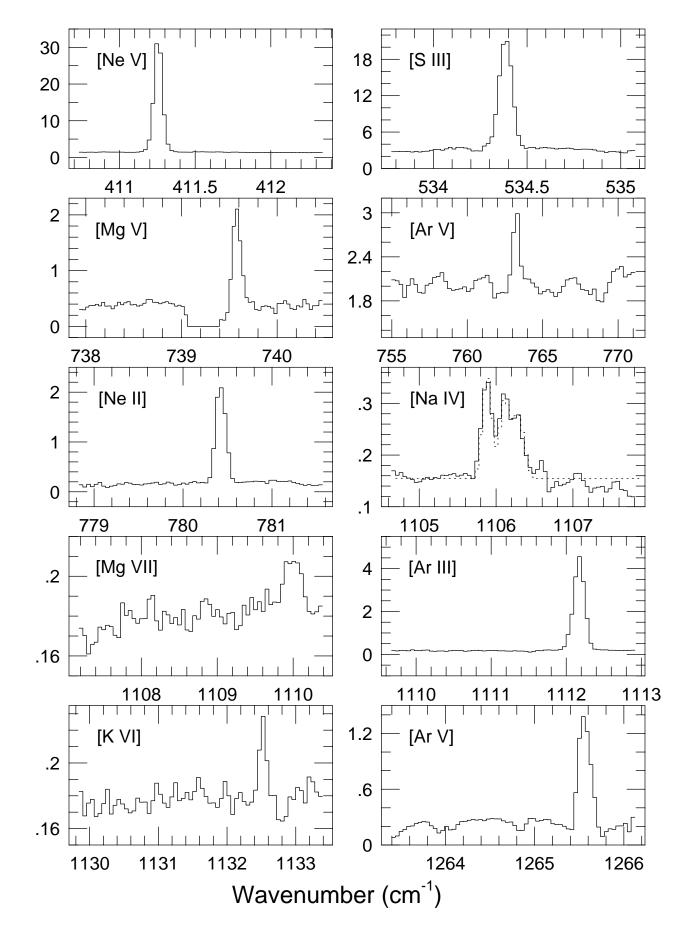
- Achtermann, J.M. 1994, PASP, 106, 173
- Aitken, D.K., & Roche, P.F. 1983, MNRAS, 202, 1233
- Baluteau, J.P., Bussoletti, E., Anderegg, M., Moorwood, A.F.M., & Coron, N. 1976, ApJ, 210, L45
- Brooke, A.L., Lambert, D.L., & Barnes, T.G. 1974, PASP, 86, 419
- Graham, J.R., Serabyn, E., Herbst, T.M., Matthews, K., Neugebauer, G., Soifer, B.T., Wilson, T.D., & Beckwith, S. 1993, AJ, 105, 250
- Greenberg, L.T., Dyal, P., & Geballe, T.R. 1977, ApJ, 213, L71
- Haas, M.R., Werner, M.W., & Becklin, E.E. 1996, in preparation
- Harvey, J.S.M. 1965, Proc.Roy.Soc.London, A, 285, 581
- Hoffleit, D., & Jaschek, C. 1982, Bright Star Catalog (New Haven: Yale Univ. Obs.)
- Kaler, J.B., & Jacoby, G.H. 1989, ApJ, 345, 871
- Kaufman, V., & Sugar, J. 1986, J. Phys. Chem. Ref. Data 15, 321
- Kelly, D.M., van der Hulst, J.M., Lacy, J.H., & Achtermann, J.M. 1995, in preparation
- Lacy, J.H., Achtermann, J.M., Bruce, D.E., Lester, D.F., Arens, J.F., Peck, M.C., & Gaalema, S.D. 1989, PASP, 101, 1166
- McClatchey, R.A., Benedict, W.S., Clough, S.A., Burch, D.E., Calfee, R.F., Fox, K., Rothman, L.S., & Garing, J.S. 1973, AFCRL-TR-73-0096.
- Roche, P.F., Aitken, D.K., Smith, C.H., & Ward, M.J. 1991, MNRAS, 248, 606
- Roelfsema, P.R., Goss, W.M., Pottasch. S.R., & Zijlstra, A. 1991, A&A, 251, 611
- Schneider, S.E., Terzian, Y., Purgathofer, A., & Perinotto, M. 1983, ApJS, 52, 399
- Townes, C.H, & Schawlow, A.L. 1955, *Microwave Spectroscopy* (New York: McGraw-Hill).
- Wiese, W.L., Smith, M.W., & Glennon, B.M. 1966, Atomic Transition Probabilities. I. H-Ne, NSRDS-NBS 4; II. Na-Ca, NSRDS-NBS 22
- Yamada, C., Kanamori, H., & Hirota, E. 1985, J. Chem. Phys., 83, 552

This preprint was prepared with the AAS IATEX macros v3.0.

Figure 1: Intensity map for the continuum-subtracted [S III] emission in NGC 7027. The contour interval is $0.172 \text{ erg s}^{-1} \text{ cm}^{-2} (\text{cm}^{-1})^{-1} \text{ sr}^{-1}$. The two contour lines in the center of the nebula denote a low flux region. North is roughly 6 degrees west of vertical in this plot. Velocities are indicated for each of the points. The velocity uncertainties are 4 km s⁻¹.

Figure 2: Dereddened spectra for the twelve emission lines detected in NGC 7027. Wavenumbers are presented in Table 1 and uncertainties are discussed in Section 3. The dotted line in the [Na IV] plot denotes our model fit for the hyperfine splitting. The [Na IV] energy splittings were determined by scaling from the hyperfine measurements of [¹⁷O I] by Harvey (1965) and from the fine-structure splittings of [O I] and [Na IV]. Relative line intensities were calculated using the formulae of Townes & Schawlow (1955). The spectrum has been convolved to have the same resolution as the [Na IV] data.





 I_v (ergs / (sec cm² cm⁻¹ sr))